

## Electrostatic screening and experimental evidence of a topological phase transition in a bulk quantum Hall liquid

Jiří J Mareš<sup>1,4</sup>, Afif Siddiki<sup>2,3</sup>, Dobroslav Kindl<sup>1</sup>, Pavel Hubík<sup>1</sup>  
and Jozef Krištofik<sup>1</sup>

<sup>1</sup> Institute of Physics of the Academy of Sciences of the Czech Republic, v.v.i., Cukrovarnická 10, 16200 Prague 6, Czech Republic

<sup>2</sup> Physics Department, Ludwig-Maximilians-Universität, Theresienstrasse 37, 80333 Munich, Germany

<sup>3</sup> Physics Department, Faculty of Arts and Sciences, Mugla University, 48170 Mugla, Turkey

E-mail: [semicon@fzu.cz](mailto:semicon@fzu.cz)

*New Journal of Physics* **11** (2009) 083028 (17pp)

Received 8 January 2009

Published 24 August 2009

Online at <http://www.njp.org/>

doi:10.1088/1367-2630/11/8/083028

**Abstract.** The electrostatic screening of a medium disordered quantum Hall liquid was investigated using an electric field penetration (EFP) technique. At sufficiently low temperatures and at magnetic fields corresponding to the integral quantum Hall regime with even filling factors, two topologically different phases of the bulk electron liquid have been identified. By means of elementary analysis of experimental data it has further been shown that the transition between these phases reveals features typical of a Kosterlitz–Thouless type phase transition. Finally, the validity of the presented physical picture has been supported by means of numerical simulations of local filling factor topography.

<sup>4</sup> Author to whom any correspondence should be addressed.

**Contents**

<b>1. Introduction</b>	<b>2</b>
<b>2. Experimental technique</b>	<b>4</b>
<b>3. Experimental results</b>	<b>7</b>
<b>4. Discussion</b>	<b>9</b>
<b>5. Numerical simulation</b>	<b>14</b>
<b>6. Conclusions</b>	<b>16</b>
<b>Acknowledgments</b>	<b>17</b>
<b>References</b>	<b>17</b>

**1. Introduction**

It is a remarkable fact that in contrast to a grounded metallic shield, a grounded two-dimensional electron liquid (2DEL), as exists at an interface between a semiconductor and an insulator, e.g. in semiconductor heterostructures, does not completely screen external quasi-static electric fields. An experimentally observed deficit of the screening ability of these systems controlled by the quantum confinement can be related either to the lack of the number of electronic states involved or to their limited accessibility for the charge carriers from the ground reservoir. Both these aspects are of primary importance especially for the understanding of the physical constitution of the quantum Hall (QH) liquid—the 2DEL in a QH regime (see below).

The solution to an electrostatic problem corresponding to the screening by a two-dimensional (2D) system is rather complicated because the electrons in the 2DEL are confined to a single 2D plane, while their electromagnetic interaction takes place mainly via a 3D surrounding space. A very effective simplification of governing equations (of the Helmholtz type) may, however, be achieved by introducing a parameter  $\lambda$ , the so-called 2D screening length [1, 2]

$$\lambda = \frac{\varepsilon\varepsilon_0}{\eta e^2}, \quad (1)$$

where  $\varepsilon\varepsilon_0$  is the permittivity and  $\eta$  the 2D density of accessible states, which at the zero temperature limit can be identified with the thermodynamic density of states, i.e.  $dn/dE_F = \eta$ . (The SI system of units is used throughout this paper.) The microphysical quantity  $\lambda$  characterizing the lateral redistribution of free charge in the 2DEL plane arising in response to the local electrostatic perturbation plays a crucial role in theory but, unfortunately, it is a concept rather inconvenient from the experimental point of view. It is therefore useful to replace it by another physical quantity more accessible to a direct experimental investigation, namely by the so-called quantum capacitance of the 2DEL of area  $A$ , which is defined as  $C_Q = \varepsilon\varepsilon_0 A/\lambda$ . The quantum capacitance  $C_Q$ , being the effective capacitance of the heterodimensional junction between the 2DEL and the 3D metallic grounded contact [3], controls the charge supply into the system that is needed for the compensation (i.e. screening) of an external applied electric field. The experimentally observable quantity  $C_Q$  thus provides a measure of the screening ability of the 2DEL characterized by the fraction of the penetrating electric field and consequently also of the microphysical parameter

$$\eta = \frac{C_Q}{Ae^2}. \quad (2)$$

As the quantities  $C_Q$  and  $A$  are easily measurable under practically all experimental conditions, we formally extrapolate the validity of relation (2) behind the approximations based on the introduction of the parameter  $\lambda$  and consider this relation to be a phenomenological definition of  $\eta$ , the density of accessible states, in systems inserted into the 2D plane even if they might not be strictly 2D. Furthermore, by means of simple general arguments it can be proved [4] that at low temperatures in a 2D electron system in the absence of magnetic field characterized by the sheet conductance  $\gamma_S$ , the quantum capacitance  $C_Q$  and  $\gamma_S$  are closely related by the formula

$$C_Q = \frac{2m\gamma_S A}{\hbar}, \quad (3)$$

where  $m$  is the effective electron mass. Accordingly, the screening properties of the 2DEL can be specified either by  $C_Q$  or by  $\gamma_S$  as well. Hence, speaking quite generally, the capacitance and transport measurements with their specific advantages and disadvantages provide complementary experimental approaches to the screening problem in 2DELs.

In the case where the 2DEL is put into a strong uniform magnetic field perpendicular to the plane where the electrons are confined, its transport and screening properties are dramatically changed. In the so-called QH regime, experimentally characterized by the vanishing of the longitudinal resistance of the electron system, the existence of a special dissipation-free electron liquid phase (QH liquid) is thus assumed, which is separated from the other bulk dissipative states by a positive mobility gap. Consequently, the electron liquid in this state may be treated as incompressible in the sense that the exchange of electrons between such a liquid and the surroundings, only at the expense of an arbitrarily small energy, is impossible. The specification of the concept of incompressibility of an electron liquid may be formulated in another way, closely related to the electrostatic screening problem, namely that the number of electrons in an incompressible electron liquid is a good quantum number with respect to an arbitrarily small perturbation of the external electric field. From this formulation it is quite clear that the presence of an incompressible phase in the 2DEL cannot alone account for its screening properties (i.e. for supplying an extra charge into the system in response to the application of the external electric field). As has been shown in a convincing way by Halperin [5], the incompressible phase in the sample in the QH regime is distributed quite inhomogeneously; the part localized in the close vicinity of edges gives rise to the non-dissipative transport channels, while the part in the bulk remains essentially non-conductive. Moreover, the complete structure of the states near the edge of the sample was found to be rather complicated, being composed of parallel well-distinguished compressible and incompressible stripes. Interestingly enough, the systems of bulk and edge states, in spite of the fact that they are physically separated, cannot be, due to the gauge invariance of the system as a whole, fully independent [6]. Theoretical models successfully describing a lot of experimentally observed features of the integer QH effect are, however, results of far reaching idealization neglecting, e.g. some aspects of disorder and irregularities of the shape of real samples. It is therefore quite likely that there are hidden effects not covered by the present theories. We believe that in highly disordered 2DEL systems, the changes of topology of compressible and incompressible regions induced by changes of temperature and magnetic field belong just to this class of phenomena.

In the regime of QH effect where the screening is rather poor because most of the bulk of the 2DEL becomes incompressible, the direct measurement of local conductivity by means of voltage probes [7] brings about relatively large disturbances (of extent up to  $\sim 10 \mu\text{m}$ ) and may not thus catch all the peculiarities of the potential profile and local density of states. In

this connection, a capacitance (e.g. EFP) technique leaving the intrinsic potential profile almost intact is obviously more feasible. On the other hand, the interpretation of EFP curves is not as easy as that of conductivity data, mainly because the theory backing this method is not well developed yet.

Evidently, a single parameter approach to the 2D screening described above can have only a limited validity in such a complex system as the QH liquid. As a matter of fact, however, in spite of extensive theoretical studies [8]–[13], only the one-parameter practically usable formulae for the non-relativistic case (i.e.  $\varepsilon\varepsilon_0 A/C_Q > \hbar/mc$ , Compton length) were worked out. Even worse is the situation in experiments, where, due to enormous technical difficulties (e.g. the necessity of absolute capacitance measurements in the fF range) only a few experimental works addressing related problems and providing unambiguous and convincing data are at our disposal [14]–[21].

The present study deals with an experimental investigation of peculiar screening properties of a disordered 2DEL in the integral QH regime (IQH plateau) corresponding to the filling factor  $\nu = 2$  and to the description of its unusual behavior, formally revealing the features analogous to the topological phase transition of Kosterlitz–Thouless type as observed, e.g. in superfluids. All the data obtained are interpreted within the frame of a simple model essentially based on the one parameter description advantageous for comparison with experiment. Finally, the resulting picture is compared with a computer simulation, which takes into account a more complete set of assumptions.

## 2. Experimental technique

First attempts at characterization of screening properties of a 2DEL by means of capacitance measurements appeared very early after the discovery of QH effects [14]. However, these pioneering investigations, based on the direct two-terminal measurement of capacitance between 2DEL and a reference electrode using a simple lock-in technique, yielded results of rather limited value due to the large stray capacitances and other parasitic effects. The essential progress has thus been made by Eisenstein *et al*, who introduced the idea to characterize the screening ability (compressibility) of the 2DEL simply by a ratio of penetrating and applied electric field. In order to obtain this ratio they actually measured the capacitance between two electrodes with a grounded 2DEL inserted in between [16, 17]. As they used for determination of capacitance a standard lock-in circuitry composed of discrete devices and also a sample with auxiliary gates, the achievable accuracy was seriously limited by stray impedances. Besides, the realization of the original idea was also not quite consequent because instead of one metallic testing electrode they used another 2DEL sheet having the same, i.e. unknown, physical nature as the system under investigation. Obviously this is the fact that inevitably complicates the interpretation of results. Therefore, in order to eliminate these imperfections we have set-up an experimental apparatus where the capacitance  $C_M$  is measured between two metallic electrodes (Hi and Lo, see figure 1), which are completely separated by the grounded 2DEL [22]. The accuracy of the whole arrangement was further essentially increased using, instead of the standard lock-in circuitry, a compact three-terminal ac capacitance transformer bridge. The main advantage of this highly sophisticated device is the possibility of complete elimination of the influence of parasitic impedances involved, provided that the two leads, Hi and Lo, are separated by a low-resistance grounded shield. Indeed, in such a case the impedance between the Hi terminal and ground diminishes the ac exciting signal but due to the tight magnetic

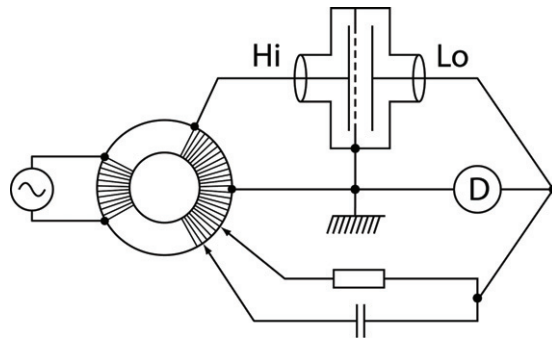


**Figure 1.** Experimental arrangement of the EFP technique exploiting an ac transformer bridge for capacitance and conductance measurements.

coupling among all the windings of the toroidal transformer, the signal supplied to the branches with resistance and capacitance standards is also diminished in exactly the same proportion, in other words, with no influence on detector reading. On the other hand, in the case where the bridge is balanced properly, that is if the ac potential difference between the ground and Lo is zero in amplitude and phase, the insertion of parasitic impedance between ground and Lo has obviously no influence on the balance of the bridge (principle of guarded measurements). Just due to these remarkable properties the accuracy of three-terminal measurements performed with transformer capacitance bridges is, as a rule, about 100 times higher than for those performed with the standard lock-in technique and even more than  $10^4$  times higher than for those made in two-terminal configuration.

For the present study, we have used the General Radio 1616 Capacitance Bridge enabling one to perform absolute capacitance measurements in the fF range with accuracy better than  $\sim 0.5\%$ . It is an important fact that this manually operated device provides inevitably not only capacitance but simultaneously also the ac conductance of the sample (analysis of ac conductance data is, however, not the subject of this paper).

For our experiments, we used standard epitaxial remotely doped GaAlAs/GaAs heterostructures (revealing the IQH effect) with a spacer thickness  $s \approx 130$  nm, a source layer with effective donor doping 2D concentration  $N \approx (3.0 - 3.7) \times 10^{15} \text{ m}^{-2}$ , and a mobility in the quantum well of about  $\sim 45 \text{ m}^2 \text{ V}^{-1} \text{ s}^{-1}$ . The details of the structure are depicted in figure 2(a). The samples were shaped into the circular mesa cutting through all epitaxial layers and provided with shadow-masked evaporated gold contacts; one contact (Lo) covers the whole area of the back of the sample, another circular one is placed at the center of the mesa and the rim of the mesa is provided with a concentric ring contact in such a way that the 2DEL is connected from the sides. As the source layer remains highly depleted at the helium temperatures, we have, in fact, to use a layered capacitor with dielectric consisting of two insulating layers with 2DEL in between. The capacitances between the Hi metallic electrode and the 2DEL ( $C_1$ ) and the Lo metallic electrode and the 2DEL ( $C_2$ ) can be very easily computed taking into account the geometry and permittivities of the system. ( $\epsilon_{\text{GaAs}} \approx 13$ ,  $\epsilon_{\text{GaAlAs}} \approx 12$ , diameter of Hi electrode 2 mm, diameter of mesa 3 mm; for thickness of particular layers, see figure 2.) For the case presented, we have obtained  $C_1 \approx 1.5 \times 10^{-9} \text{ F}$  and  $C_2 \approx 2.6 \times 10^{-12} \text{ F}$ . The accuracy of the computation was checked by means of direct measurement of the capacitance of the structure with the 2DEL disconnected from the ground. In such a case, the 2DEL

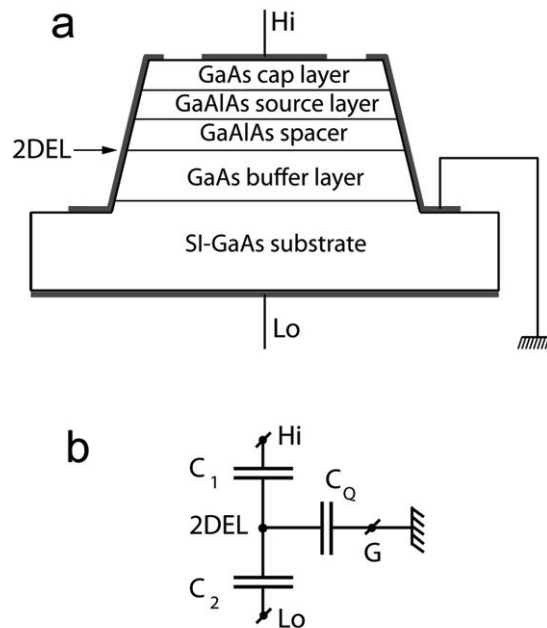


**Figure 2.** Structure and contact configuration of the Corbino sample used for EFP measurements (a). Thicknesses of particular layers were: substrate  $320 \mu\text{m}$ , buffer layer  $700 \text{ nm}$ , spacer  $130 \text{ nm}$ , source layer  $80 \text{ nm}$  and cap layer  $20 \text{ nm}$ . Intended donor concentration in the source layer was  $2 \times 10^{24} \text{ m}^{-3}$ , other layers were nominally undoped. Equivalent circuit approximating the behavior of the sample (b).

serves as a conductive stratum and the resulting capacitance  $C$  should correspond to the serial combination of  $C_1$  and  $C_2$ , namely,  $C^{-1} = 1/C_1 + 1/C_2$ . As the direct experiment provided the value  $C \approx 2.8 \times 10^{-12} \text{ F}$ , we consider our computations to be essentially correct. It is further apparent that both high (Hi) and low (Lo) metallic electrodes, as well as the 2DEL, are integral parts of one sandwich sample. In such an arrangement, the Hi–Lo capacitance measured with grounded 2DEL,  $C_M$ , is the direct measure of the fraction of electric field that penetrates through the 2DEL. The relation between the quantum capacitance  $C_Q$  of the 2DEL screen and the measured capacitance  $C_M$  follows from an elementary analysis of the equivalent circuit used (see figure 2(b)) and is given by a formula

$$C_Q = C_1 C_2 (1/C_M - 1/C_2), \quad (4)$$

where the empirical constants  $C_1$  and  $C_2$  have the meaning already specified above. The formula for the evaluation of  $C_Q$  thus reads:  $C_Q = 1.82 \times 10^{-21} (1/C_M - 3.85 \times 10^{11}) \text{ F}$ .

The testing electric field was applied only to the central part of the bulk 2DEL lying just below the high (Hi) electrode, while its perimeter was grounded so that the system had effectively Corbino disc topology, which is a fact that is very important for the interpretation of the results. The measurements themselves were performed in the temperature range  $1.2\text{--}4.2 \text{ K}$  and in perpendicular magnetic fields up to  $\sim 8 \text{ T}$ . The ac signal of the bridge had frequencies tunable in the range  $10^2\text{--}10^5 \text{ Hz}$  and a voltage of  $\sim 0.01 \text{ V}$  resulting in a testing electric field of  $\sim 30 \text{ V m}^{-1}$ , which was proved to be in the range where both the capacitance and the conductance were field independent.

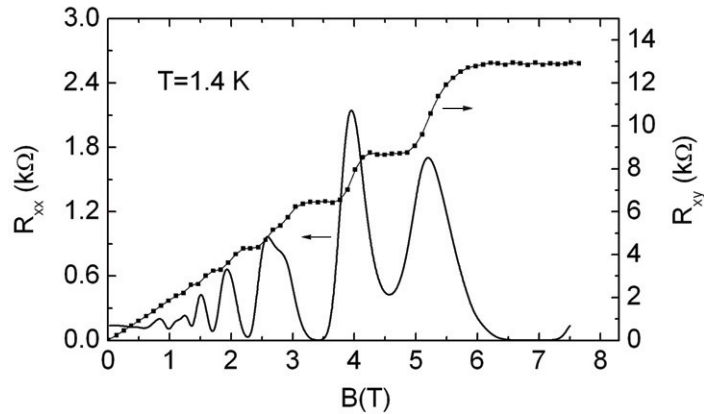


**Figure 3.** An example of longitudinal ( $R_{xx}$ ) and Hall resistance ( $R_{xy}$ ) measured on heterostructures used for EFP studies.

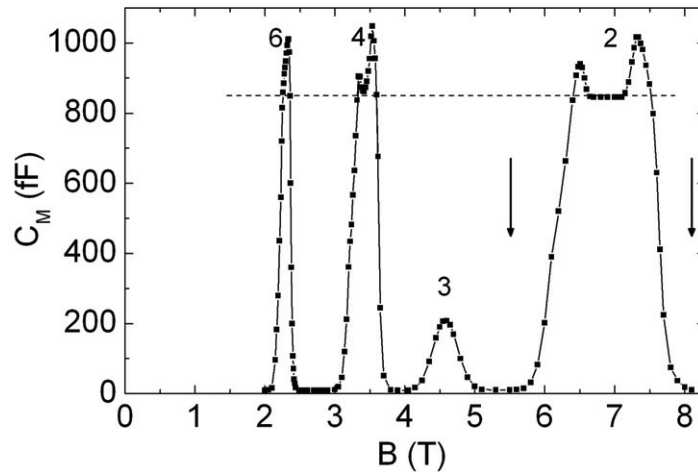


**Figure 4.** An example of the EFP curve taken at a temperature of 1.3 K and at a measuring frequency of 1.05 kHz plotted in terms of capacitance  $C_M$  measured between points Hi and Lo. The peaks are labeled by filling factors  $\nu$ . The arrows correspond to the edges of the IQH plateau for  $\nu = 2$  obtained at the same temperature.

### 3. Experimental results

Prior to the EFP measurements, in order to characterize the transport properties of our heterostructures, we also prepared from the same wafers samples having a standard Hall bar configuration [23]. An example of the dc magnetotransport measurement performed in one of these samples is shown in figure 3. It is apparent that it behaves as a typical medium-mobility 2DEL system clearly revealing all the features of IQHE. These curves enabled us to determine also the positions of the edges of IQH plateaus corresponding to  $\nu = 2$ , which are, for better orientation, marked on the EFP curves by arrows.

A representative example of the dependence of the EFP signal taken at a temperature of 1.3 K and a frequency of 1.04 kHz with the magnetic field applied perpendicularly to the 2DEL and plotted up to filling factor  $\nu = 6$  is depicted in figure 4. The well resolved peaks are

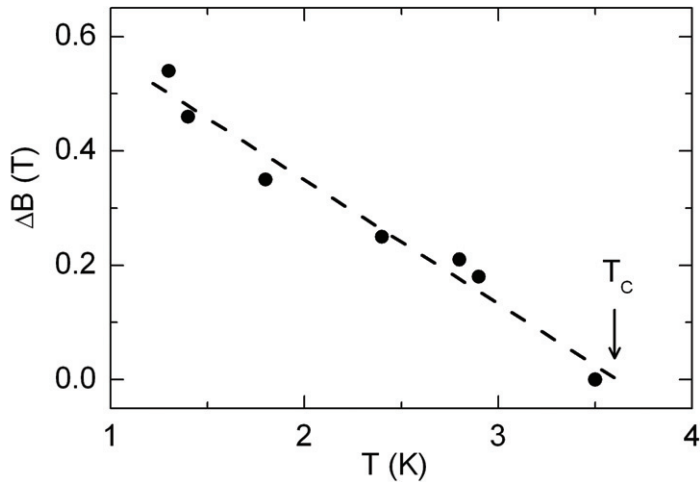


**Figure 5.** Width  $\Delta B$  of the flat part of the EFP curve observed near the center of IQHE plateau depicted as a function of temperature.

positioned just at the centers of the IQH plateaus but their widths (full-width at half-maximum (FWHM)) are markedly smaller. It can be further shown that the width of the gaps  $\delta B$  between the following even peaks scales with the filling factor as  $\nu \propto \sqrt{\delta B}$  in full agreement with a classical model of the Landau level broadening [11]. Besides, there is a fairly constant baseline at  $C_M \approx 13$  fF (i.e.  $C_Q \approx 1.4 \times 10^{-7}$  F) in between the peaks, which is very likely due to the screening by a fully degenerate 2DEL having the state density  $\eta \approx m/\pi\hbar^2 = 1.8 \times 10^{36} \text{ J}^{-1} \text{ m}^{-2}$  (effective mass  $m \approx 0.067 \times m_e$ ). The very property of the 2DEL revealed by this EFP curve is the following one. At a frequency of  $\sim 1$  kHz and at sufficiently low temperatures ( $\leq 1.8$  K), the even peaks do not exceed the common limit at  $C_M \approx 1.2 \times 10^{-12}$  F, which is appreciably lower than the capacitance of the sample measured with the 2DEL completely disconnected from the ground (floating stratum). In this case, the capacitance of the sample was of purely geometrical origin and had a value of  $\sim 2.6 \times 10^{-12}$  F. This fact proves without ambiguity the existence of a residual screening (or, in other words, the existence of radial currents) due to the 2DEL in the IQH regime with  $\nu = 2, 4, 6$ , etc. Using equations (2) and (4), one obtains the result that this residual screening should correspond to the reduction of  $\eta$  and consequently also of the effective electron density to  $\sim 1\%$  of the original baseline value, which is assumed to be approximately equal to the donor concentration  $N \approx 3.3 \times 10^{15} \text{ m}^{-2}$ . The peaks themselves have no single maximum but have a characteristic additional structure that is most apparent for the peak at  $\nu = 2$ . (Although only this case is discussed further, the same arguments are valid also for other even values of  $\nu$ .) This peak is split into two well-distinguished peaks with a flat valley in between. While the position of the bottom of this valley is, within limits specified below, perfectly temperature and frequency independent ( $C_{M0} = 0.83 \text{ pF} \pm 0.5\%$ ), its width increases with the decreasing temperature and/or increasing frequency, which shifts both the side peaks toward the edges of the IQH plateau. This behavior is illustrated in figure 5, where the temperature dependence of the width of the valley is plotted. Parts of the EFP curves corresponding to the center of the plateau are for two different temperatures depicted in figure 6 in coordinates  $\eta$  versus  $B$ . The shapes of the side extremes were proved to be sensitive to the details of the contacting technology that brings in ill-controlled amounts of impurities, deep



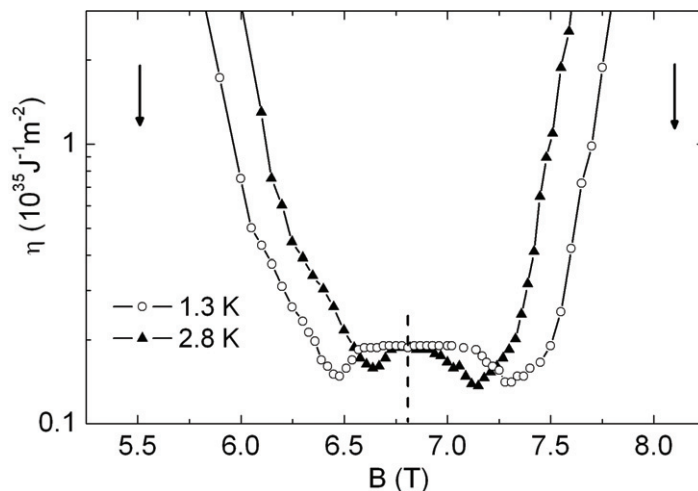


**Figure 6.** The EFP peak (filling factor 2, measuring frequency 1.05 kHz) measured at two different temperatures and plotted in  $\eta$  versus  $B$  coordinates. For evaluation of effective density of states  $\eta$  from experimental data equation (2) was used.

defects and additional disorder in the sample. Such a view is supported also by the fact that the other symptoms of metastability typical of the presence of deep centers, e.g. disappearance of some details of the first-run curve, were systematically observed. As for the peaks with odd values of  $\nu$ , they were many times smaller than even peaks and in most cases merged with the baseline. An exception was the peak with  $\nu = 3$  the height of which reached about 20% of the saturated height of even peaks.

The existence of the region within the peaks with even  $\nu$  where the EFP signal is constant and equal to the common value  $C_{M0}$  is, as we believe, an experimental fact of primary importance. This flat part of the EFP curve positioned just at  $C_{M0}$  only appears when the sample is cooled down to a temperature of  $\sim 3.5$  K and with decreasing temperature its width further increases. In the same temperature range peaks with odd filling factors, which e.g. at 4.2 K merge with the baseline, also start to develop. Qualitatively similar influence on the shape of the peak as the lowering of temperature below  $T_C \approx 3.5$  K, namely, the enlargement of the flat central part of the peak and simultaneous appearance of odd peaks, was seen for the increase of measuring frequency from 30 Hz up to 100 kHz. It has, however, quite a different effect on the baseline, which with frequency increasing above  $\sim 3$  kHz starts to rise upward so that eventually, at measuring frequencies  $> 30$  kHz, the whole EFP curve becomes practically flat apparently approaching the limiting constant value of  $C_{M0}$ .

#### 4. Discussion

The observed behavior is evidently in contradiction with standard models of the IQH effect (for reviews see [24, 25]). By standard models we mean the bulk [26] (disorder and localization based) and the edge models [5, 12]; however, our results are consistent with the ‘screening theory’ of the IQH effect [27]. Accordingly, in the IQH regime, the 2DEL undergoes reconstruction into a system of compressible and incompressible strips parallel to the edges of the sample (Chklovskii–Shklovskii’s stripes [8]). In the Corbino structure, the equalizing

currents supplying the extra screening charge into the bulk of the 2D system from its grounded periphery thus have to pass continuous incompressible rings at the edge of the 2DEL, i.e. to overcome the spectral gap of the incompressible phase. In such a case, the Fermi level is positioned between two adjacent Landau levels where only strictly localized states exist, which excludes coherent transport. Consequently, the screening should be either totally absent or due to another type of incoherent transport, which is possible only at finite temperatures. While such a model is admissible for the explanation of the behavior near the edges of the EFP peak, it can in no way account for the structure of its central part.

In order to make clear such complex and rather unexpected behavior of the EFP signal an essentially single-parameter model was developed, which provides quantitative estimates of electrostatic screening for different positions of the Fermi level with respect to the ladder of Landau levels in the 2D system. The kernel of the model presented is based on the relations between the density of accessible states at the Fermi level  $\eta$  and amplitudes of disorder-induced fluctuating potential, an item that should be discussed first.

The role of the disorder in a traditional approach to the IQH effect is, as a rule, limited only to the conditions necessary for the bare existence of the QH plateau, i.e. breaking of the translation invariance, broadening of Landau levels and smoothing of the edge potential [24, 25]. It can be shown, however, that the disorder introduced by the random distribution of impurities in the source layer that is inevitably present in all 2D structures revealing the IQH effect, may in some cases be sufficient to deform the system of the Landau levels in such a way that their amplitude of variation is comparable with their energy distance. Indeed, the amplitude  $w_0$  of long-range potential fluctuations can be determined assuming that they are due to the Coulomb interaction [23] of unscreened donors in the source layer. Taking further into account the fact that the donors are non-correlated, because they were incorporated into the lattice at very high temperature, the most probable distance between neighboring ionized donors in the source layer with effective donor concentration  $N$  can be computed by means of Hertz's formula [28]. The resulting amplitude  $w_0$  representing the Coulomb interaction over this distance thus reads

$$w_0 = \left( \frac{e^2}{\varepsilon \varepsilon_0} \right) \sqrt{\frac{N}{8\pi}}. \quad (5)$$

In our case ( $\varepsilon \approx 13$ ), this quantity providing an overall energy scale for disorder-induced phenomena is approximately  $w_0 \approx 2.6 \times 10^{-21}$  J (16 meV), which is comparable with the Landau level splitting in GaAs at 6.7 T,  $\hbar\omega \approx 1.9 \times 10^{-21}$  J ( $\approx 12$  meV). The amplitude  $w$  of potential fluctuations present in the plane of the 2DEL (i.e. the actual width of the impurity induced energy band), which is a superposition of random harmonics of the source layer potential, is essentially given by  $w_0$  multiplied by the aspect ratio  $\lambda/2s$  (cf [9]), where  $2s$  is the distance between the source layer and its electrostatic image in the 2DEL. The formula for  $w$  then reads

$$w = \frac{\sqrt{N/32\pi}}{\eta s}. \quad (6)$$

According to the last equation, the width of the impurity induced potential profile should change appreciably with the variation of the density of accessible states in the vicinity of the Fermi level, which is for the moment taken here as an independent parameter tuned by external means (e.g. by magnetic field). Large  $\eta$ , which is of the order of one particle 2D density of states ( $\eta_0 \approx m/\pi\hbar^2$ ), provides a sufficient electron density to ensure that the valleys of the potential profile lying below the Fermi level are completely filled with electrons and thus effectively

smoothed. The spatial distribution of electrons in the 2DEL is, in this case, inhomogeneous but the potential profile is quite flat with negligible variation. With decreasing  $\eta$  the concentration of electrons at the Fermi level also diminishes and their number is not sufficient to equalize all irregularities of the induced potential profile, which thus becomes more pronounced. This process continues until the density of accessible states reaches a certain critical value  $\eta_C$  at which the complete denudation of the potential profile characterized by the condition  $w \approx w_0$  takes place. At this significant point  $\eta_C$  can be estimated as

$$\eta_C = \frac{\varepsilon \varepsilon_0}{2s e^2} \quad (7)$$

and the corresponding concentration of electrons within the impurity induced band as

$$n_C = \frac{\sqrt{N/32\pi}}{s}. \quad (8)$$

We claim that the relations just derived fit very well the behavior actually observed in the central part of the IQH plateau. The density of states  $\eta$  evaluated by means of formula (2) from the experimental dependence of  $C_Q$  on the magnetic field (see figure 6) reaches in this region a constant value of  $\sim 1.9 \times 10^{34} \text{ J}^{-1} \text{ m}^{-2}$ , which is very near to the rough estimate of  $\eta_C \approx 1.7 \times 10^{34} \text{ J}^{-1} \text{ m}^{-2}$  made on the basis of equation (7). These figures together with the estimate for  $n_C \approx 4.4 \times 10^{13} \text{ m}^{-2}$  also excellently account for the observed reduction in the screening ability of the 2DEL in the IQH plateau to  $\sim 1\%$  with respect to the baseline value ( $\eta \approx 1.8 \times 10^{36} \text{ J}^{-1} \text{ m}^{-2}$ ,  $\eta \approx 3.3 \times 10^{15} \text{ m}^{-2}$ ).

In order to explain the observed features of the EFP peak in its complexity together with its relation to the IQH curve, let us now follow the behavior of the EFP signal step by step with an increasing magnetic field accompanied by the corresponding shift of the Fermi level (see again figure 1). Approaching the IQH plateau from the low  $B$  side, the EFP signal keeps the baseline value of  $C_M$ , which provides practically the same estimate for  $\eta$  as the theoretical one-particle 2D density of states mentioned above ( $m/\pi \hbar^2 = 1.8 \times 10^{36} \text{ J}^{-1} \text{ m}^{-2}$ ). Hence, the variation of the disorder-induced potential is quite negligible along the 2DEL ( $w \approx 0.15 \text{ meV}$ ) and the corresponding thickness of the heterodimensional junction characterized by the 2D screening length ( $\lambda \approx 2.5 \times 10^{-9} \text{ m}$ , according to equation (1)), is so small there that the contact can be regarded as an ideal tunnel contact [29]. Consequently, here we have to deal with a process where an almost flat 2D Landau level with  $p = 3$  ( $p$  means the ordinary number of Landau level counted upward from the lowest one) is incident with the Fermi level and is ideally connected with the external 3D metallic reservoir.

In the following part of the EFP peak (ranging from 5.5 to 5.8 T) near to the edge of the IQH plateau, the Fermi level should be, according to the classical approach, somewhere within the tail of localized states positioned just below the Landau level ( $p = 3$ ). Then currents can flow only along the edges of the sample where the Fermi level cuts the Landau level with  $p = 2$  and the only flow allowed in the Corbino ring topology is an azimuthally quasi-persistent current. On the other side, our experiment shows that the radial currents necessary for the relaxation of the external polarization of the 2DEL in the Corbino structure does co-exist in this part with the IQH plateau. The only explanation of this fact is that the decrease of  $\eta$  (and consequently of electron concentration) actually manifested by a slight increase of  $C_M$  above the baseline (corresponding to  $\lambda \approx 3 \text{ nm}$ ) is not sufficient for the considerable suppression of the electron scattering from the contact onto the Landau level ( $p = 3$ ) in the interior of the 2DEL. Moreover, even a relatively small increase in the variation of a long-range potential profile in the

interior of the 2DEL ( $w \approx 0.6$  meV) due to the electron depletion is helpful for the preservation of the coherent transport along this extended Landau level because of its local lowering to, or below the Fermi level. In other words, we propose that in this part of the EFP curve corresponding to the position of the edge and the beginning of the IQH plateau ( $\nu = 2$ ) the extra carriers can be supplied from the 3D metallic contact onto the perturbed Landau level ( $p = 3$ ) lying in the interior of the 2DEL by the scattering through the heterodimensional junction of thickness  $\sim \lambda$ .

It is clear that such a process is very likely if the localization radius of the wavefunctions in the 2DEL represented by the magnetic length  $l = \sqrt{\hbar/eB}$  is larger than  $\lambda$ . In the opposite case  $l \leq \lambda$ , the situation has to change dramatically. The transport of carriers onto the disturbed Landau level ( $p = 3$ ) being controlled by the tunneling over the distance of the screening length  $\lambda$  should be exponentially damped with increasing ratio  $\lambda/l$  and thus strongly temperature and frequency dependent [29]. We are convinced that just such a tunneling-controlled mechanism of disconnection of the bulk 2DEL from the contact with an increasing magnetic field is responsible for the steep increase of the EFP curve observed between 5.8 and 6.5 T. The plausibility of such an explanation also supports the fact that the estimates for screening and magnetic lengths at a point where the EFP curve starts to markedly deviate from the baseline ( $B = 5.85$  T,  $C_M = 55$  fF) are practically identical ( $\lambda \approx 1.07 \times 10^{-8}$  m and  $l \approx 1.06 \times 10^{-8}$  m).

The same process limiting the charge supply into the bulk of the 2DEL, however, results simultaneously in its depletion followed by the denudation of the potential profile in which large-scale potential fluctuations start to develop. Some of these fluctuations extending to the close vicinity of the contact create in regions where the Fermi level cuts the deformed Landau levels new transport channels that can supply the electrons from the ground into the interior of the 2DEL. In effect, the screening ability of the system is improved in spite of further decrease in the number of free electrons involved and the process should be accompanied by decrease of  $C_M$  which is actually observed between 6.5 and 6.6 T. The process being controlled by the large-scale potential fluctuations is of statistical nature; nevertheless, it depends on details of the donor distribution in a source layer near to the periphery of the 2DEL. This fact accounts for the observed sensitivity of the shape of local maxima on the EFP curve to the contact technology and also for the metastability of samples in these regions.

According to our opinion, the most interesting part of the EFP curve is the flat valley near the center of the Hall plateau (between 6.6 and 7.1 T in figure 2), which is very likely the manifestation of a topological phase transition taking place in the disordered QH liquid. In order to be more specific, let us note first the very nature of Landau levels, i.e. their vortex character is closely related to the axial properties of the field, accompanied by translational symmetry, which is broken down only at the boundary of the 2DEL. As we have already shown above, the electron depletion in the Hall regime leads to the denudation of the potential profile (the limit  $n \approx n_C$ ) and to the appearance of random large-scale potential fluctuations introducing into the bulk of the 2DEL new boundary conditions at the Fermi level which are very similar to a physical boundary. The final result of such a process is that the Landau levels cannot preserve their long-range translational symmetry. The number of dephasing channels per  $\text{m}^2$ , which remain in the  $kT$  band at the Fermi level crossing the deformed system of Landau levels can be in such a case counted using the obvious expression  $mkT/2\pi\hbar^2$ . This quantity should, however, simultaneously coincide with the number of electrons per  $\text{m}^2$  admissible by the disorder intrinsically involved in the structure. Taking thus into account the fact that the upper limit for this concentration is given by formula (8), we can make the following estimate

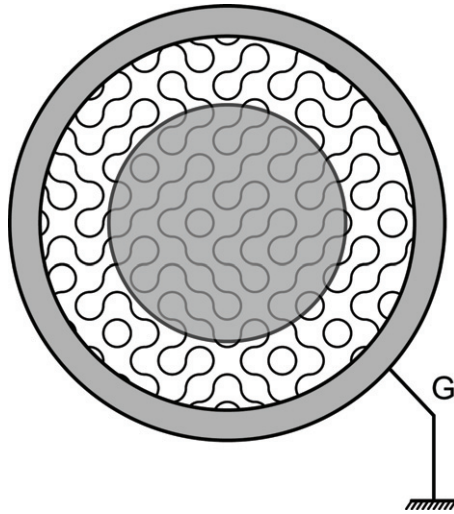


**Figure 7.** An idealized view of a Corbino disc capacitor showing the ‘dragon paths’ allowing the electrostatic screening in the IQHE low temperature regime.

for the critical temperature  $T_C$  below which the translational symmetry of Landau levels in the 2D bulk is lost, namely:

$$T_C = 2\pi\hbar^2 n_C / mk. \quad (9)$$

Remarkably, this formula that is formally identical to the Kosterlitz–Thouless criterion for topological phase transition in superfluid helium films [30], also controls the onset of appearance of the flat valley on the EFP curve. Indeed, substituting for  $n_C = 4.4 \times 10^{13} \text{ m}^{-2}$  and for  $m = 0.067 \times m_e$ , i.e. the values already used above, we obtain for  $T_C = 3.65 \text{ K}$ , which is in nice agreement with our experiment yielding  $T_C \approx 3.6 \text{ K}$  (see figure 5). These facts strongly support the following scenario. Electron depletion of the 2DEL near the center of the Hall plateau diminishes the effectiveness of screening there and, consequently, enables in the bulk of the system development of large-scale potential fluctuations with amplitude comparable to the distance between the consecutive Landau levels. At the intersection of the Fermi level with these Landau levels (with  $p = 2$  and  $3$  for  $\nu = 2$ ) copying the random potential profile then leads to a system of Chklovskii–Shklovskii’s stripes creeping along the potential hills and valleys into the bulk of the 2DEL. As the width of these stripes is confined to Larmor’s length [8] ( $\sim me/4\pi\epsilon\epsilon_0\hbar B \approx 8.5 \text{ nm}$  at  $6.8 \text{ T}$ ) characterizing the extent of the wavefunction, the network of such compressible current-bearing regions in the essentially incompressible 2D bulk of the 2DEL, which is responsible for remnant screening of the system, must be effectively 1D. It is obvious that our scenario resembles very closely the Chalker–Coddington model [31] of disordered 2DEL according to which the compressible 1D stripes, reflecting the random structure of potential fluctuations, creep into the bulk of the 2DEL in the form of ‘dragon paths’ having the character of Peano’s self-affine curves [32]. A somewhat idealized picture of this model for the Corbino disc configuration is depicted in figure 7.

In order to support such an opinion by complementary arguments it should be added that in the depleted state which is characterized by the condition  $\eta \rightarrow \eta_C$ , the electrons having concentration as low as  $n_C$  are incident only with the impurity induced strongly oscillating potential profile and thus cannot continuously reach all the points in the 2DEL plane. The

electrons are thus made to create a new phase bound to the compressible network of dimension  $<2$ . The fact that to a certain extent the screening is invariant with respect to the changes of temperature, measuring frequency and external magnetic field actually means that it is insensitive to the redistributions of electron wavefunctions over this phase. Expressing this fact in terms of topology, we can state that the new phase is invariant with respect to continuous mappings. According to Brouwer's theorem [33], however, claiming that the integer (topological) dimension is topologically invariant, the compressible network has to keep its topological dimension which can be thus equal to only 1. Interpreting this result we can again, as above, conclude that in our case we have to deal with the topological<sup>5</sup> phase transition between the diluted, highly disordered 2DEL and the irregular network of compressible 1D channels.

Let us now approach the interpretation of the high field side of the EFP peak. Further increase in the magnetic field shifts the undisturbed position of the Landau level with  $p = 2$  nearer to the Fermi level, bringing about the enhancement of electron population there. Consequently, the impurity induced large-scale potential profile is smoothed again, the system of 1D quantum channels connecting the interior of the system with the contact disappears and the continuity of large regions of the 2DEL is restored. This process should manifest itself by an increase of  $C_M$ , quite resembling that actually observed on the EFP curve between 7.1 and 7.3 T. The enrichment of the system by electrons due to the decrease of the gap between the Fermi level and the Landau level  $p = 2$  has, however, also another effect, namely, the shortening of the screening length  $\lambda$  controlling the tunneling probability between the contact and the disturbed Landau level ( $p = 2$ ) representing the 2DEL. The combination of both these effects is responsible for the existence of a local maximum on the EFP curve at 7.3 T which is followed by a steep decrease of  $C_M$  with increasing magnetic field. Such a decrease can obviously continue only until the screening (i.e. tunneling) length  $\lambda$  approaches the natural localization limit given by the magnetic length  $l$  at  $\sim 7.9$  T ( $l \approx 9.1 \times 10^{-9}$  m,  $\lambda \approx 7.9 \times 10^{-9}$  m). At this point, the EFP curve reaches practically its baseline and we have again to deal with the case where the charge necessary for the screening is supplied via an ideal low-impedance contact on the Landau level ( $p = 2$ ).

Summarizing, the model presented being compatible with the classical theory of the QH liquid can simultaneously account satisfactorily for the observed behavior of the EFP signal. Moreover, the quantitative relations involved, being originally intended to be only order-of-magnitude estimates, approximate the actual parameters of the experimentally observed EFP curve remarkably well.

## 5. Numerical simulation

In order to test further the plausibility of our model it should be compared either with direct mapping of the topography of a QH fluid [34] or with a corresponding computer simulation. From these two possibilities the latter one has been realized. For this purpose, the ready-made self-consistent scheme developed for the study of potential and/or filling factor distribution in a disordered QH liquid was used [35, 36]. By means of this scheme it was e.g. possible to follow the changes in topology of the electron liquid during the sweeping of magnetic field

<sup>5</sup> Let us recall that a topological change is meant to be any change of topological invariants characterizing the system, e.g. its connectivity, dimension, etc.

through the Hall plateau. Mainly on the basis of practical grounds the computer simulations were performed on a relatively small but macroscopic square part of the 2DEL having an area of  $2\ \mu\text{m} \times 2\ \mu\text{m}$ . For the simulation of realistic boundary conditions, the circular gate electrode of diameter  $1\ \mu\text{m}$  was put into the center of the sample. To be explicit with the boundary conditions, we assumed periodicity in both directions, i.e.  $V(x=0, y) = V(x=2\ \mu\text{m}, y)$  and  $V(x, y=0) = V(x, y=2\ \mu\text{m})$ . Such a treatment of the boundary conditions is justified, since the central region we are interested in is far away from the physical boundaries of the sample, where Ohmic contacts reside. It is known that in the close proximity of such metallic contacts, the ‘edge’ incompressible strips form because of the bending of the bare confinement potential [36]. Besides the confinement and external gate potential, the random component of the potential was simulated by insertion of an ensemble of Gaussian impurities. Meanwhile, the collision broadened Landau levels are represented by semi-elliptic functions, for the sake of consistency, which are obtained from the self-consistent Born approximation [2, 27]. The broadening parameter ( $\gamma_B = \Gamma_B/\hbar\omega_c = 0.1$ ) is chosen such that the Landau levels do not overlap and the resulting mobility is intermediate. The corresponding parameters controlling this random component, i.e. the impurity concentration in the source layer and spacing between the source layer and the 2D subsystem, were chosen to be the same as in the real experiment ( $N = 3.3 \times 10^{15}\ \text{m}^{-2}$ ,  $s = 130\ \text{nm}$ ). We are convinced that the use of the small area sample is not restricting because, due to the self-affinity of the problem, any process taking place in a small section of the system has to have the essential features of the process taking place in the whole scaled-up system as well. It is necessary to note that the variation of the amplitude of the disorder-induced potential reduces drastically when considering nonlinear screening in the presence of magnetic field. The screened potential is given by

$$V^q = \frac{V_{\text{ext}}^q}{\varepsilon(q)}, \quad (10)$$

where  $\varepsilon(q)$  is the momentum ( $q$ ) dependent Thomas–Fermi dielectric function and  $V_{\text{ext}}^q$  is the external potential in  $q$ -space. The surface density  $Q_0$  of the induced charge is then  $Q_0 = e^2\eta_0 V_{\text{ext}}^q/\varepsilon(q)$ . For large  $q$ , i.e. for the long-range fluctuations, the potential is well screened; a rough estimate shows that the amplitude is reduced 40 times, in contrast to the short-range part that remains almost unchanged. A detailed investigation of the screening properties and their relation to the IQH effect can be found in [37]. We thus start our calculations by initializing the random impurity distribution, then calculate the ‘screened’ impurity potential from equation (10) and finally initiate the self-consistent calculations in the presence of an external magnetic field.

The results of the computer simulation in terms of the local filling factor for magnetic fields increasing in 0.2 T steps from 6 to 7.4 T are depicted in figure 8, where the gray areas represent the regions with exact integer filling factor  $\nu = 2$ . Other filling factors may be identified using the attached color scale. This series of figures clearly demonstrates the transition from the situation where the edge states (a–c) percolate to the central part of the situation where the edge states are shared by bulk states (d–f). Moreover, it is evident that figure 8(e) corresponds to the appearance of a section of compressible ‘dragon path’ (in yellow) penetrating through the incompressible (gray) region underneath the central gate electrode. We can thus see that the computer simulation repeated the essential features of the model used for the interpretation of EFP data.

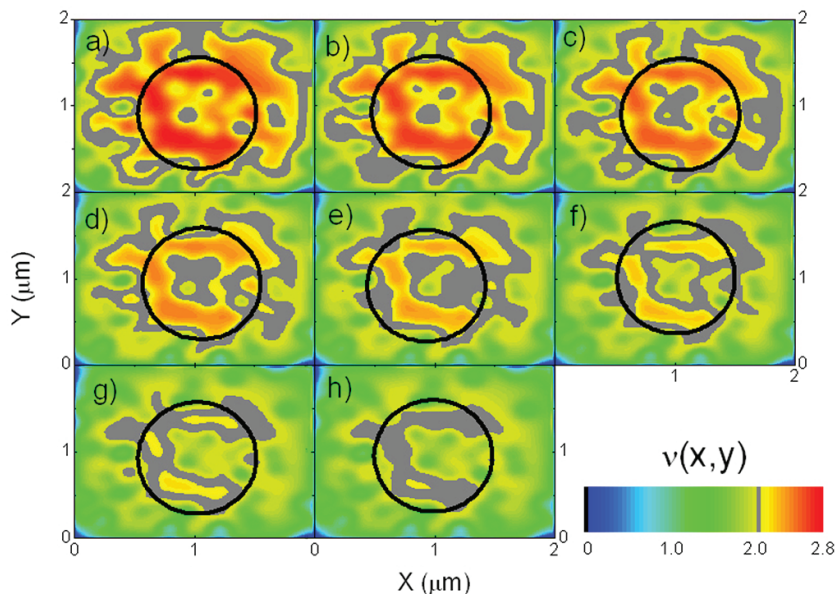


**Figure 8.** Results of computer simulation of the distribution of local filling factor depending on external magnetic field. The values of magnetic fields corresponding to separate figures are: (a) 6.0 T, (b) 6.2 T, (c) 6.4 T, (d) 6.6 T, (e) 6.8 T, (f) 7.0 T, (g) 7.2 T, (h) 7.4 T. The simulation was performed on a  $2 \mu\text{m} \times 2 \mu\text{m}$  area of 2DEL; the diameter of the central gate electrode was  $1 \mu\text{m}$ .

## 6. Conclusions

In conclusion, measuring the 2D density of accessible states using the EFP technique, we have proved that in the region of the IQH plateau ( $\nu = 2$ ) two qualitatively different screening mechanisms can be distinguished. For the interpretation of this finding a simple model has been developed. The essential part of this model is a semi-quantitative description of disorder-induced potential fluctuations, which are according to our present knowledge an inevitable part of any real 2D semiconductor system. From comparison of our experimental data with the figures provided by the model we have concluded that the former mechanism taking place at the edges of the EFP peak is very likely due to the tunneling of electrons from the contact into the interior of the 2DEL over a distance given by the 2D screening length  $\lambda$ . The latter mechanism operating in the central part of the IQH plateau is then probably due to the existence of the ‘dragon paths’—1D quantum channels with compressible electron fluid percolating throughout the impurity induced potential profile into the bulk of the system. As a result, we have shown the possibility to interpret the phenomenon as a particular case of the topological phase transition of Kosterlitz–Thouless type in a disordered 2D electron system driven by external magnetic field. The plausibility of such an interpretation was also confirmed by computer simulation clearly visualizing the changes in the topography of the local filling factor during this transition.



## Acknowledgments

This work has been mainly supported by the grant agencies of the Czech Republic and of the Academy of Sciences (Projects No. 202/07/0525 and No. A1010404), whereas numerical studies were financially supported by NIM Area A and SFB 631.

## References

- [1] Shik A Y 1995 *Semiconductors* **29** 697
- [2] Ando T, Fowler A B and Stern F 1982 *Rev. Mod. Phys.* **54** 437
- [3] Luryi S 1988 *Appl. Phys. Lett.* **52** 501
- [4] Mareš J J, Krištofik J and Hubík P 2002 *Physica E* **12** 340
- [5] Halperin B I 1982 *Phys. Rev. B* **25** 2185
- [6] Fröhlich J, Pedrini B, Schweigert C and Walcher J 2001 *J. Stat. Phys.* **103** 527
- [7] Ahlswede E, Weitz P, Weis J, von Klitzing K and Eberl K 2001 *Physica B* **298** 562
- [8] Chklovskii D B, Shklovskii B I and Glazman L I 1992 *Phys. Rev. B* **46** 4026
- [9] Efros A L 1999 *Phys. Rev. B* **60** 13343
- [10] Cooper N R and Chalker J T 1993 *Phys. Rev. B* **48** 4530
- [11] Apalkov V M and Raikh M E 2003 *Phys. Rev. B* **68** 195312
- [12] Büttiker M 1992 *Nanostructured Systems—Semiconductors and Semimetals* vol 35 ed M Reed (New York: Academic) p 191
- [13] Levitov L S, Shtyov A V and Halperin B I 2001 *Phys. Rev. B* **64** 075322
- [14] Smith T P, Goldberg B B, Stiles P J and Heiblum M 1985 *Phys. Rev. B* **32** R2696
- [15] Templeton I M 1987 *J. Appl. Phys.* **62** 4005
- [16] Eisenstein J P, Pfeiffer L N and West K W 1992 *Phys. Rev. Lett.* **68** 647
- [17] Eisenstein J P, Pfeiffer L N and West K W 1994 *Phys. Rev. B* **50** 1760
- [18] Oto K, Takaoka S and Murase K 2001 *Physica B* **298** 18
- [19] Oto K, Sanuki T, Takaoka S, Murase K and Gamo K 2002 *Physica E* **12** 173
- [20] Arai K, Hashimoto S, Oto K and Murase K 2003 *Phys. Rev. B* **68** 165347
- [21] Pusep Yu A, Chiquito A J, Arakaki H and de Souza C A 2007 *Physica E* **40** 2682
- [22] Mareš J J, Krištofik J and Hubík P 1999 *Phys. Rev. Lett.* **82** 4699
- [23] Mareš J J, Feng X, Koch F, Kohl A and Krištofik J 1994 *Phys. Rev. B* **50** 5213
- [24] Prange R E and Girvin S M 1990 *The Quantum Hall Effect* (Heidelberg: Springer) p 12
- [25] Chakraborty T and Pietiläinen P 1995 *The Quantum Hall Effects* 2nd edn (Berlin: Springer) p 26
- [26] Kramer B, Kettemann S and Ohtsuki T 2003 *Physica E* **20** 172
- [27] Siddiki A and Gerhardts R R 2004 *Phys. Rev. B* **70** 195335
- [28] Hertz P 1909 *Math. Ann.* **67** 387
- [29] Henisch H K 1984 *Semiconductor Contacts* (Oxford: Clarendon) p 319
- [30] Thouless D J 1998 *Topological Quantum Numbers in Non-relativistic Physics* (Singapore: World Scientific) p 102
- [31] Chalker J T and Coddington P D 1988 *J. Phys. C: Solid State Phys.* **21** 2665
- [32] Mandelbrot B B 1983 *The Fractal Geometry of Nature* (New York: W H Freeman)
- [33] Brouwer L E J 1911 *Math. Ann.* **70** 161
- [34] Finkelstein G, Glicofridis P I, Ashoori R C and Shayegan M 2000 *Science* **289** 90
- [35] Siddiki A and Marquardt F 2007 *Phys. Rev. B* **75** 045325
- [36] Arslan S, Cicek E, Eksi D, Aktas S, Weichselbaum A and Siddiki A 2008 *Phys. Rev. B* **78** 125423
- [37] Siddiki A and Gerhardts R R 2007 *Int. J. Mod. Phys. B* **21** 1362